IEICE TRANSACTIONS

on Electronics

This advance publication article will be replaced by the finalized version after proofreading.

Convergence Characteristics of Domain Decomposition Method for Full-Wave Electromagnetic Analysis

Toshio MURAYAMA[†] *and* **Amane TAKEI**[††], *Members*

SUMMARY   A domain decomposition method is widely utilized for analyzing large-scale electromagnetic problems. The method decomposes the target model into small independent subdomains. An electromagnetic analysis has inherently suffers from late convergence analyzed with iterative algorithms such as Krylov subspace algorithms. The DDM remedies this issue by decomposing the total system into subdomain problems and gathering the local results as an interface problem to adjust to achieve the total solution. In this paper we report the convergence properties of the domain decomposition method while modifying the size of local domain and the region shape on several mesh sizes. As experimental results show, the convergence speed depends on the number of interface problem variables and the selection of the local region shapes. In addition to that the convergence property differs according to the target frequencies. In general it is demonstrated that the convergence speed can be accelerated with large cubic subdomain shape. We propose the subdomain selection strategies based on the analysis of the condition numbers of the governing equation.
key words: *Finite element method, Domain decomposition method, Iterative algorithm, Convergence characteristics*

1.   Introduction

The large-scale electromagnetic (EM) analysis is successfully utilized to the geometrically complicated product design, wireless communication or EMC analyses[1]. Several numerical approaches have been proposed and utilized to analyze these issues. The Finite Difference Time Domain (FDTD) method is one of the popular algorithms which has been applied to large-scale EM problems[2]. The FDTD algorithm is heavily utilized for many cases because of its versatile and easiness to implement as a software. In addition to that nature, the FDTD method can be effectively parallelized with multi-core processors and can be applied to the large-scale problems. The algorithm, however, has critical limitations that the analysis region should be partitioned into rectangular blocks. Also the algorithm takes vast amount of time steps for low frequency problems due to the Courant-Friedrichs-Lewy condition. The Finite Difference Frequency Domain (FDFD) method is the algorithm for frequency domain, however, it has the same limitation as the rectangular elements[3]. Since the FDFD method is required to solve the matrix equation, some kind of ingenuity is required when it is applied to the large-scale EM problems. The Moment method is another widely used scheme

for antenna and waveform propagation analyses[4]. Its advantage is the relatively small number of unknown variables required for solving the problem. The equation composed by the moment method is, however, dense and requires huge calculation costs. It also requires the special treatment to analyze the model including the dielectric materials. The Finite Element Method (FEM) is versatile and flexible algorithm for solving time and frequency EM problems. It has been applied widely applicable to the complex structure and large-scale problems. It is difficult, however, to solve the problem when the size of the system becomes large. Furthermore the EM problems inherently suffer from slow convergence due to the null space of rotation operator [5][6][7]. $A - \phi$ method is one of the countermeasure to this problem[8]. However, large-scale problems still need breakthrough for the practical analysis. The multigrid methods[9][10] have been attracting attention and utilized over various problem domains especially for the elliptic problems[11]. It also has parallel effective nature[12] and can be processed in parallel. It generates the hierarchical coarse grids to correct global errors[13] while basic iterative method reduces short-wavelength error. Many studies have shown the methods are very effective, however, there are some cases that it is difficult to generate 'coarse grids' accurately for complex electromagnetic problems[14].

The Domain Decomposition Method (DDM) [15][16][17] is one of the countermeasures to overcome the large-scale problems[18]. The method divides the target problem into small subdomains which are solved independently as smaller size problem shown in Fig. 1. These results are assembled to generate the entire solution and hence can solve the large-scale problems. It can be applied to many engineering domain such as the thermal analysis [19] and can treat not only frequency domain but also time domain EM problems[20]. Most domain decomposition methods can be categorized into the two classes. One is the Schwarz methods which divides the total region into the overlapping subdomains. Another class is based on the Schur complement method which is regarded as the non-overlapping subdomains. We focus on the non-overlapping DDM since the overlapping DDM requires communications between subdomains which become dominant when the number of subdomains increases which can be a disadvantage for an extra large-scale analysis[21]. For the DDM preconditioning methods [22] or domain aware decomposition methods were recently proposed[23] since it is critical for the method to generate optimal number of subdomain variables and shape[24]. The 3D planer decompo-

[†]The author is with the University of Tokyo, Tokyo, 113-8564 Japan
[††]The author is with the University of Miyazaki, Miyazaki, 889-2192 Japan

sition is also proposed[25]. However, there are less studies reported for the DDM with rectangular meshes and shape of the subdomain dependencies. Under these circumstances, it seems to be worthwhile investigating the characteristics of the DDM algorithm. In this paper the convergence characteristics of rectangular meshes are newly reported. The characteristics with different size models when the number of subdomains and shapes are modified are fully discussed and the fast convergence strategy is proposed. Optimal memory and calculation resources required for the DDM are also discussed and reported.
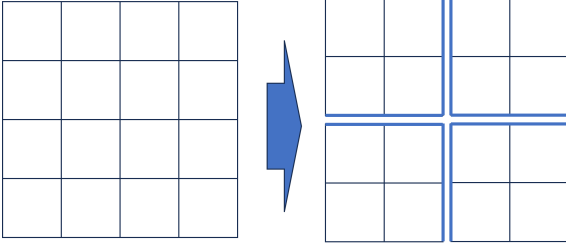

Fig. 1 Domain decomposition method. Bold edges are interface edge elements and others are inner edges.

2. FEM Formulation with Edge Elements

A 3D EM problem is formulated and discretized with edge elements from the vector Helmholtz equation as follows [7] [11]:

$$\nabla \times \frac{1}{\mu_r} \nabla \times \vec{E} + j\omega\mu_0\sigma\vec{E} - \omega^2\mu_0\epsilon_0\epsilon_r\vec{E} = -j\omega\mu_0\vec{J_v} \quad (1)$$

where $\vec{E}$ is the electrical field intensity vector, μ_0 and μ_r are the permeability of free space and relative permeability, respectively, ϵ_0 and ϵ_r are the permittivity of free space and relative permittivity, respectively, σ is conductivity ω is angular frequency and $\vec{J_v}$ is an excitation current vector. By expanding $\vec{E}$ with edge elements $\vec{\omega_{e,i}}$ we obtain the following discretized system of equations

$$Mx = -j\omega f \quad (2)$$

where

$$M_{ij} = \iiint_\Omega \nabla \times \vec{\omega_{e,i}} \cdot \frac{1}{\mu_r} \nabla \times \vec{w_{e,j}} dv$$

$$+ j\omega\mu_0 \iiint_\Omega \vec{\omega_{e,i}} \cdot \sigma\vec{\omega_{e,j}} dv - \omega^2\epsilon_0\mu_0 \iiint_\Omega \vec{\omega_{e,i}} \cdot \epsilon_r\vec{\omega_{e,j}} dv \quad (3)$$

$$f_i = \mu_0 \int \vec{w_{e,i}} \cdot \vec{J_v} dv. \quad (4)$$

Here, M is a sparse symmetric complex matrix. In order to analyze the open region electromagnetic waveform scattering problems, the finite region must be enclosed by a radiation condition or absorbing boundary layers. Many approaches are proposed for the radiation condition. In our

implementation the perfectly matched layers (PML) are employed to absorb the outgoing waveform.

3. Domain Decomposition Method

The domain decomposition is a very broad research subject and has received intensive attention in the advent of parallel computation[21]. In this paper we divide the analyzed model into non-overlapping subdomains. Equation (2) is divided into the following form

$$\begin{pmatrix} M_{aa} & M_{ab} \\ M_{ba} & M_{bb} \end{pmatrix} \begin{pmatrix} x_a \\ x_b \end{pmatrix} = j\omega \begin{pmatrix} f_a \\ f_b \end{pmatrix} \quad (5)$$

where M_{aa} corresponds to the internal edge elements contained in the subdomains. By eliminating x_a we obtain a reduced system for the unknowns on the interface edge elements as

$$(M_{bb} - M_{ba}M_{aa}^{-1}M_{ab})x_b = j\omega(f_b - M_{ba}M_{aa}^{-1}f_a). \quad (6)$$

In order to reduce the required memory, usually M_{aa} is chosen as a set of small diagonal blocks which correspond to the subdomains as follows:

$$M_{aa} = \begin{pmatrix} M_{00} & 0 & \dots & 0 \\ 0 & M_{11} & \dots & 0 \\ \vdots & \vdots & \ddots & \vdots \\ 0 & 0 & \dots & M_{n-1,n-1} \end{pmatrix}. \quad (7)$$

By assembling the subdomains as a block diagonal matrix, M_{aa} is easily factorized as upper and lower triangle matrices as $M_{aa} = L * U$ with modest memory resources, and can be used to calculate instead of M_{aa}^{-1}.

3.1 Iterative Algorithms

A system of linear matrix equation is solved by direct methods and iterative methods. The former algorithms directly modify the matrix to be solved and obtain solution within finite calculation operations. Some studies try to develop direct solution of large-scale EM problems[26]. However, when the size of the equation becomes large, it takes vast amount of memory and calculation resources. Therefore it is not suitable for a large-scale problem.

Iterative algorithms such as Krylov subspace methods are heavily used for large-scale problems[27]. COCG[28] or COCR[29] and their derivation schemes [30][31] are commonly applied to the EM problems since the governing equations are symmetric complex matrices. The COCG algorithm is expressed as shown in Fig. 2. In the DDM algorithm, the matrix vector product Ap_j is performed as $(M_{bb} - M_{ba}M_{aa}^{-1}M_{ab})p_j$ where M_{aa}^{-1} is replaced by LU substitution.

3.2 Characteristics of the Reduced System

The reduced system (6) becomes the smaller size matrix and relatively easier to be solved by the iterative algorithms.

$$r_0 \Leftarrow b - Ax_0$$
$$p_0 \Leftarrow r_0$$
$$For \; j = 1, \cdots, m \; Do :$$
$$\quad \alpha = \frac{(r_j, \bar{r}_j)}{(Ap_j, \bar{p}_j)}$$
$$\quad x_{j+1} \Leftarrow x_j + \alpha_j p_j$$
$$\quad r_{j+1} \Leftarrow r_j - \alpha_j Ap_j$$
$$\quad \beta_j = \frac{(r_{j+1}, \bar{r}_{j+1})}{(r_j, \bar{r}_j)}$$
$$\quad p_{j+1} \Leftarrow r_{j+1} + \beta_j p_j$$
$$\quad If \; converged \; Stop.$$

Fig. 2   COCG algorithm [32].

The Krylov subspace iterative methods take much iterations when the condition number $\kappa(M)$ of the matrix is large[32]. The reduced matrix has a smaller condition number compared with that of the original system as depicted in Fig. 3 where the target model consists of 10x10x10 meshes with size of 1mm operating at 1GHz frequency. This fact means
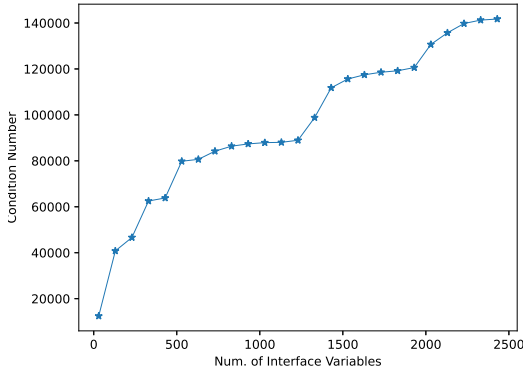

Fig. 3   Condition numbers of reduced matrices.

that when the number of subdomain variables increases, the number of the interface variables decreases since they correspond to the remainder after subtracting the subdomain variables from the overall variables. As a result the condition of the reduced system becomes better and the equation converges faster. In order to verify this we performed several numerical experiments.

4.   Comparison of Convergence Characteristics

Numerical experiments have been done to investigate the convergence properties with three models shown in Fig. 4 (Mesh I through III). They consists of 160x160x160 cubic elements backed by 16-layer perfectly matched layers. We choose the number of PML layers with margin for our purpose according to the results shown in [21] where 10-layer PML shows enough performance. Each model has the excitation source located at the center of the model. The sources are single frequency sinusoidal current sources. Mesh sizes are $\frac{\lambda}{60}$, $\frac{\lambda}{300}$ and $\frac{\lambda}{600}$ where λ is a wavelength of an electromagnetic wave. Experimental statistics are shown in Table

Table 1   Simulation statistics.

Num. of elements	4,096,000
Num. of freedom	12,134,800
Absorbing boundary condition	16 Perfectly matched layers unless otherwise specified
Element type	Brick Nédélec 1st order
Element size	5mm × 5mm × 5mm (Mesh I)
Element size	1mm × 1mm × 1mm (Mesh II)
Element size	0.5mm × 0.5mm × 0.5mm (Mesh III)
Operation frequency	1Ghz
Convergence criterion	Relative error < 1e-6
Platform	AMD EPYC 7502 32-Core
Numerical library	Intel oneAPI Math Kernel Library [33]

1. The subdomain sizes which mean the number of x, y and z meshes applied to the Model I through III are shown in Table 2.

Table 2   Subdomain sizes applied to the models.

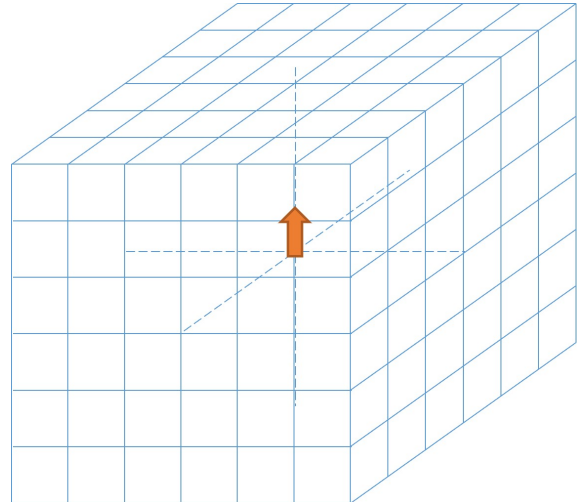| Subdomain size	Total number of variable	The number of variables in interface problem
10x10x10	12,134,800	2,042,880
20x20x20	12,134,800	1,044,960
40x40x40	12,134,800	453,600
80x80x80	12,134,800	152,160

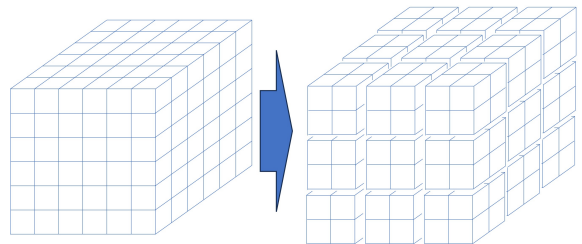**Fig. 4**   Target model. It consists of 160x160x160 cubic elements.

Fig. 5   DDM model decomposition with cubic subdomain.

Table 3 Required iteration counts.

Model	Subdomain size			
	10x10x10	20x20x20	40x40x40	80x80x80
$\frac{\lambda}{60}$	3,530	2,050	2,014	1,112
$\frac{\lambda}{300}$	2,732	1,588	951	1,013
$\frac{\lambda}{600}$	1,571	1,318	662	733

The DDM algorithm is applied to the simulation models with COCG algorithm where the models are decomposed into cubic subdomains shown in Fig. 5. The convergence profiles are shown in Fig. 6.

4.1 Iteration Counts

First, the iteration counts required to converge to the approximation solution are shown. Three models are solved with different number of subdomain size 10x10x10, 20x20x20, 40x40x40 and 80x80x80 (Table2). According to these results the algorithm converges within less iteration counts when the number of subdomain variables is larger (Table3). There are minor exceptions that the model with 40x40x40 subdomains are a little faster than one with 80x80x80 subdomains in Mesh II and Mesh III, which are almost the same number of iterations. As the number of subdomain variables becomes large, the number of interface problem variables decreases. As for the effect of the number of subdomain variables it can be said that generally speaking the smaller the number of variables in the interface problem, the smaller the required iteration count becomes.

4.2 Mesh Size dependency

The difference of the mesh size corresponds to the operation frequency when the size of the mesh is normalized. In our previous report[34] the convergence rate of Krylov subspace methods has dependency on the operation frequency. In this time's cases, when the size of the mesh is smaller, which corresponds to the low frequency operation, the DDM converges in fewer iterations. Over the Mesh I through III the DDM converges in fewer iterations according to the number of subdomain variables. This is because when the number of subdomain variables increases, the variables in the interface problem decreases resulting in good condition of the governing matrix.

4.3 Memory Resources

In Fig. 7 it is shown that the subdomain size increases, the required memory resources increase. The main part of the memory consumption is a *LU* factorization of the internal variables. When formulated with edge elements with the hexahedron meshes there are 1 diagonal and up to 32 off-diagonal elements in one line of the governing equation matrix. The expected required memory resource are roughly estimated with the band matrix with the size of 33. According to the numerical experiments, the required memory roughly proportional to $O(n^{1.2 \sim 1.3})$ where n is the number of unknowns.

4.4 Calculation Cost

As discussed above, the DDM completes the analysis within small iteration counts when the number of interface variables is smaller. On the other hand, it takes much calculation costs when solving $M_{aa}^{-1} \times r$ at one iteration in COCG process. The required total simulation time is the product of the time of one iteration and the number of the iteration count for convergence. The elapsed times for the convergence in our experiments are shown in Fig. 8. It was shown that the total required time is minimal around 20x20x20 subdomains over Mesh I through Mesh III models. Even if the number of interface problem variables is smaller, the total required simulation time may increase. This means that there are optimal number of subdomain variables which depends on the problem characteristics. In our experiments when the size of the subdomain variables increases, it takes $O(n^{1.2 \sim 1.3})$ larger computational costs which cannot be compensated by the iteration count acceleration by large subdomain size.

4.5 Subdomain Shape Dependency

Until here, we discussed the DDM properties with cubic subdomain decomposition. However, it is possible to select subdomains as a rectangular parallelepiped. In this subsection the effect of different shape of the subdomains is considered. Two cases are experimented where the number of the subdomain variables and the interface variables are almost the same but the shapes are cubic and planer rectangular parallelepiped (Fig. 9). The required memory resource for decomposition are almost the same when the number of the internal variables are nearly equal. It is clear that the models with cubic subdomains is much faster than those with rectangular parallelepiped. In Fig. 10 the required memory resources for the different subdomain shapes are shown. It is depicted that the rectangular parallelepiped subdomain requires less memory compared to the cubic shape when the number of subdomain variables are almost same. Also, the parallelepiped subdomain does not consume twice as much memory as the cubic subdomain whose number of subdomain variables is almost half of the parallelepiped. In Mesh I with the rectangular subdomain did not converge within 10,000 iterations(Fig. 11).

This fact reveals that the shape of the subdomain strongly affects the convergence characteristics. Although much more experiments will be required to determine the optimal subdomain shape, however, it is a better strategy to select the shape of the subdomain as nearly as the cubic form even though the condition number of the flat decomposition is better and the required memory is less in comparison with the cubic one.

5. Discussion

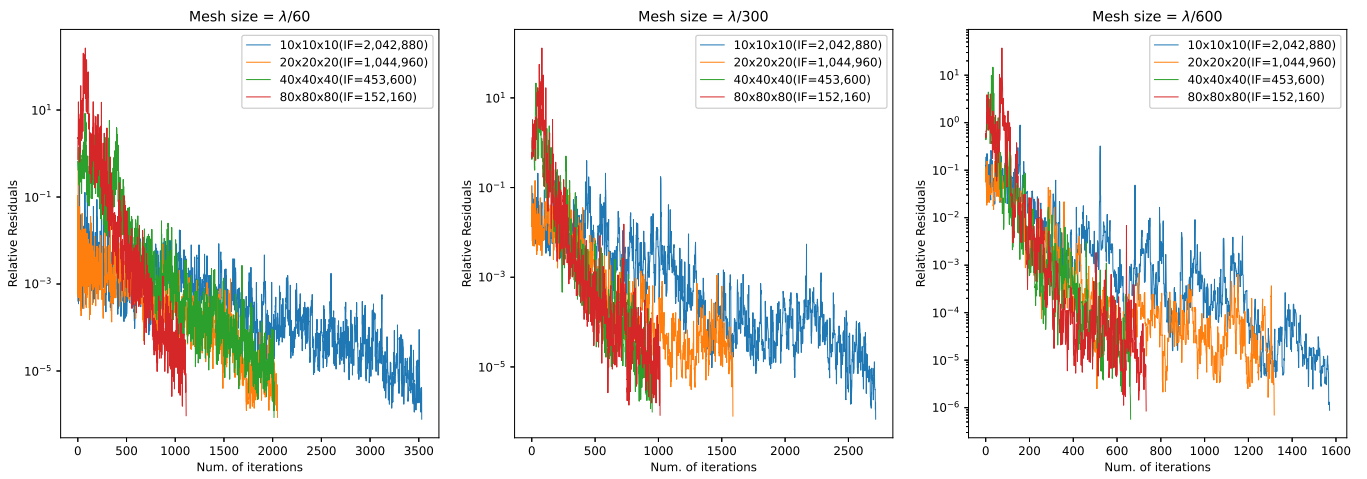According to the results of our numerical experiments, It is

Fig. 6   Convergence Profiles of Different Mesh Size. ("IF" in the graphs means the number of interface variables.)
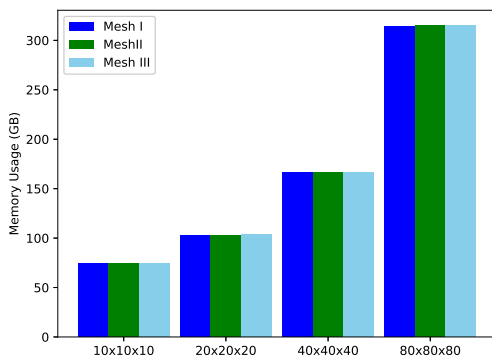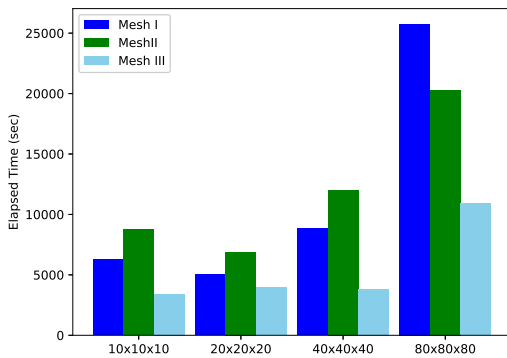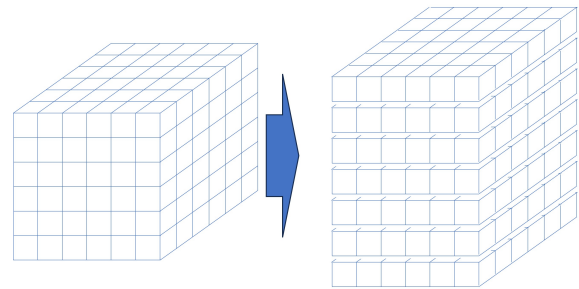

Fig. 7   Memory consumptions.

Fig. 9   Flat Decomposition.

Fig. 8   Execution time (elapsed)
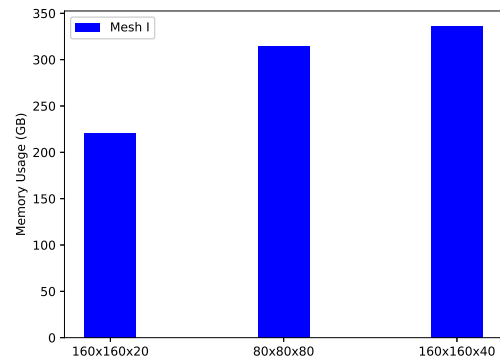
Fig. 10   Required memory resources for the different shapes.

clear that the DDM is robust and effective algorithm for the EM problems. It converges all cases with different size of the meshes. It is a beneficial strategy that the subdomains are selected as cubic shape and its size is chosen depending on the experimental results for the fast convergence.

The operation frequency affects the convergence property and the lower the frequency the faster the iteration convergence in our cases. However, there should be optimal frequency and this requires more experiments in various fre-
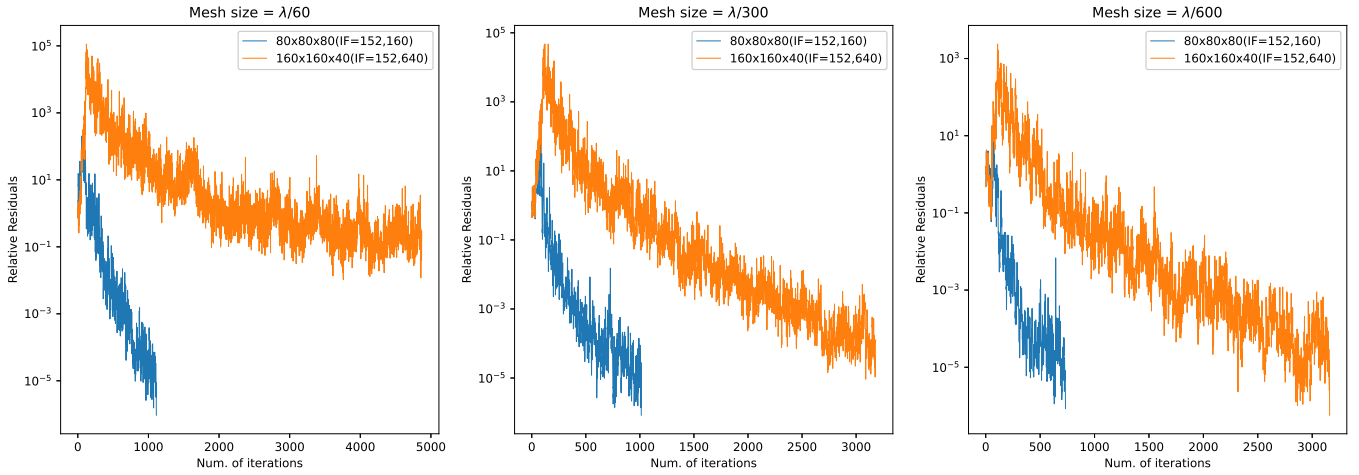
Fig. 11 Convergence profiles of different subdomain shape models. ("IF" in the graphs means the number of interface variables.)

quencies. It seems that the lower the operation frequency becomes, the fewer the DDM iteration requires for convergence (Table 3). The elapsed time of Mesh II, however, takes more than that of Mesh I in many cases (Fig. 8). This reversal phenomenon is due to the calculation costs required to solve the subdomain with a direct sparse matrix solution algorithm. The direct matrix solver performs pivoting for the required accuracy and fill-ins occur differently according to the frequency. The optimized mesh size for the specified operation frequency depends on these factors and it will be possible to obtain empirical rules through more numerical experiments.

It was shown that the shape of the subdomains affects the convergence characteristics. In our cases, the cubic subdomain is effective than that of the rectangular parallelepiped.
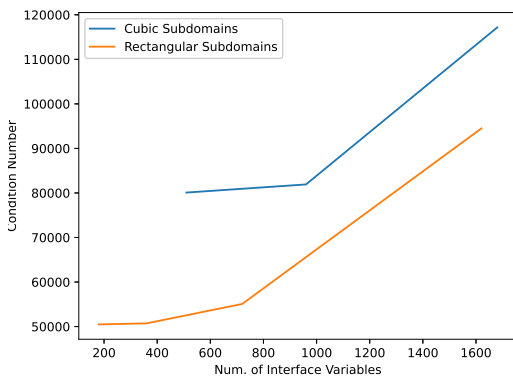

Fig. 12 Condition numbers with cubic and flat subdomains.

As shown in Fig. 12 the condition number decreases according to the number of interface problem variables. In

these results, the flat decomposes have smaller condition numbers which is not compatible with the convergence profile in Fig.11. This means that the condition number is not strongly related to the upper bound of the iteration count when the subdomain shapes are different. However, the tendency to decrease and saturate of the condition number is verified useful and the condition number can be a good indicator when the model is composed of the same subdomain shapes.

6. Conclusions and Future Work

In this paper we make it clear that the convergence properties of the DDM applied to the electromagnetic full-wave analyses with rectangular mesh edge elements. It is also clarified that the convergence speed can be accelerated by increasing the number of subdomain which leads to the decrease of the number of interface variables. The strategy for selecting the subdomain size is proposed in accordance with condition number of the governing matrix. Generally the required number of iterations has a negative correlation to the number of interface variables, however, the more the number of variables in the subdomains increases, the more the memory resources are required. The properties with different subdomain shapes are also investigated. It is shown that the convergence rate largely depends on the shape of the subdomain. Frequency dependencies are also studied. The convergence ratio differs on the analysis frequency, however, the required iteration counts depend on the iterative algorithms and need more studies on this issue. Therefore the frequency dependency should be studied more in detail. In this report the DDM converges faster when the operation frequency is lower, however, the convergence characteristics depends on the frequency and it also differs with the kind of Krylov subspace algorithms. The optimal frequency of the DDM with the interface size, subdomain shape and

the iteration algorithms will be the next study themes. In this paper we use structured lattice for the numerical experiments, however, the DDM can be applied to the unstructured meshes such as tetra elements. We will further study the convergence properties in case of unstructured meshes.

References

[1] A. Takei, S. Sugimoto, M. Ogino, S. Yoshimura, and H. Kanayama, "EMC analysis in a living environment by parallel finite element method based on the iterative domain decomposition method," Theoretical and Applied Mechanics Japan, vol.62, pp.237–245, 2014.

[2] A. Taflove, Computational Electrodynamics : The Finite-Difference Time-Domain Method, Artech House, 1995.

[3] T. Watanabe and H. Asai, "Macromodel generation for hybrid systems consisting of electromagnetic systems and lumped RLC circuits based on model order reduction," IEICE Transactions on Fundamentals, vol.E87-A, pp.398–405, Febrary 2004.

[4] W.C. Gibson, The Method of Moments in Electromagnetics, Chapman and Hall/CRC, 2007.

[5] R. Hiptmair and J. Xu, "Auxiliary space preconditioning for edge elements," IEEE Transactions on Magnetics, vol.44, no.6, pp.938–941, June 2008.

[6] T. Murayama and S. Yoshimura, "Fast electromagnetic simulation with superimposed multigrid preconditioner," IEICE Transactions on Communications, vol.J92-B, pp.1449–1456, January 2009.

[7] T. Murayama, A. Takei, and S. Yoshimura, "Fast full-wave electromagnetic simulation by multiplicative Schwarz preconditioning with alternating direction node blocks," IEICE Transactions on Electronics, vol.J93-C, pp.647–656, December 2010.

[8] T. Iwashita, T. Mifune, S. Moriguchi, and M. Shimasaki, "Physical meaning of the advantage of A-phi method in convergence," IEEE Transactions on Magnetics, vol.45, pp.1424–1427, March 2009.

[9] D.N. Arnold, R.S. Falk, and R. Winther, "Multigrid in H (div) and H (curl)," Numerische Mathematik, vol.85, no.2, pp.197–217, 2000.

[10] A. Aghabarati and J.P. Webb, "An algebraic multigrid method for the finite element analysis of large scattering problems," IEEE Transactions on Antennas and Propagation, vol.61, no.2, pp.809–817, Feb 2013.

[11] Y. Zhu and A. Cangellaris, Multigrid Finite Element Methods for Electromagnetic Field Modeling, Wiley-IEEE Press, 2006.

[12] Y. Hirotani, T. Mifune, T. Iwashita, T. Murayama, and H. Ohtani, "Large-scale high-frequency electromagnetic finite element analysis using the parallel geometric multigrid method," IEICE Transactions on Communications, vol.J93-B, pp.1331–1341, September 2010.

[13] A. Ida, T. Iwashita, T. Mifune, and Y. Takahashi, "Variable preconditioning of Krylov subspace methods for hierarchical matrices with adaptive cross approximation," IEEE Transactions on Magnetics, vol.52, no.3, pp.1–4, March 2016.

[14] T. Iwashita, Y. Hirotani, T. Mifune, T. Murayama, and H. Ohtani, "Large-scale time-harmonic electromagnetic field analysis using a multigrid solver on a distributed memory parallel computer," Parallel Computing, vol.38, pp.485–500, 2012.

[15] A. Takei, S. Yoshimura, and H. Kanayama, "Large-scale analysis of high frequency electromagnetic field by hierarchical domain decomposition method," IEEJ Transactions on Fundamentals and Materials, vol.128, pp.591–597, Sep. 2008.

[16] A. Takei, S. Sugimoto, M. Ogino, S. Yoshimura, and H. Kanayama, "Full wave analyses of electromagnetic fields with an iterative domain decomposition method," IEEE Transactions on Magnetics, vol.46, no.8, pp.2860–2863, Aug 2010.

[17] A. Takei, M. Ogino, and S.I. Sugimoto, "High-frequency electromagnetic field analysis by cocr method using anatomical human body models," Transactions on Magnetics, vol.54, no.3.

[18] L. Yin and W. Hong, "A fast algorithm based on the domain decomposition method for scattering analysis of electrically large objects,"

Radio Science, pp.1–9, Jan. 2002.

[19] X. Zhang and M. Tang, "Non-conformal domain decomposition method for thermal analysis of integrated packages," IEEE 10th Asia-Pacific Conference on Antennas and Propagation (APCAP), pp.1–2, 2022.

[20] I. Massaoudi and P. Bonnet, "A non-overlapping time domain decomposition method," International Conference on Electromagnetics in Advanced Applications (ICEAA), pp.612–612, 2023.

[21] J.M. Jin, The Finite Element Method in Electromagnetics, Third Edition, Wiley-IEEE Press, 2014.

[22] H. Kanayama, M. Ogino, S.Sugimoto, and Q. Yao, "A preconditioner construction for domain decomposition analysis of large scale 3d magnetostatic problems," Fourth International Conference on Modeling, Simulation and Applied Optimization, pp.1–4, 2011.

[23] Q. Lim, H.W. Gao, and Z. Peng, "Full-wave simulation of a 10,000-element reconfigurable intelligent surface with a single workstation computer," IEEE International Symposium on Antennas and Propagation and USNC-URSI Radio Science Meeting (USNC-URSI), pp.587–588, 2023.

[24] S. Sun and D. Jiao, "Split-field domain decomposition parallel algorithm with fast convergence for electromagnetic analysis," IEEE Journal on Multiscale and Multiphysics Computational Techniques, pp.135–146, 2023.

[25] H. Wang, L. Xu, J. Yin, H. Liu, X. Li, and B. Li, "A 3d planar partitioning method for finite element domain decomposition method," IEEE International Symposium on Antennas and Propagation and USNC-URSI Radio Science Meeting (USNC-URSI), pp.1–2, 2023.

[26] N. Lochner, D.G. Makris, and M.N. Vouvakis, "Low rank direct finite element solvers," IEEE International Symposium on Antennas and Propagation and USNC-URSI Radio Science Meeting (USNC-URSI), pp.45–46, 2023.

[27] T. Sogabe, Iterative Methods for Sparse Linear Systems, Second Edition, Springer, 2023.

[28] H.A. van der Vorst and J.B.M. Melissen, "A Petrov-Galerkin type method for solving Axk=b, where A is symmetric complex," IEEE Transactions on Magnetics, vol.26, no.2, pp.706–708, Mar 1990.

[29] T. Sogabe and S.L. Zhang, "A COCR method for solving complex symmetric linear systems," J. Comput. Appl. Math., vol.199, no.2, pp.297–303, February 2007.

[30] X.M. Gu, T.Z. Huang, L. Li, H.B. Li, T. Sogabe, and M. Clemens, "Quasi-minimal residual variants of the COCG and COCR methods for complex symmetric linear systems in electromagnetic simulations," IEEE Transactions on Microwave Theory and Techniques, vol.62, no.12, pp.2859–2867, Dec 2014.

[31] M. Ogino, A. Takei, and S. Sugimoto, "Performance evaluation of finite element analysis for high frequency electromagnetic fields using the MINRES-like_CS method," IEICE technical report, vol.116, no.212, pp.77–80, 2016.

[32] Y. Saad, Iterative Methods for Sparse Linear Systems, Second Edition, SIAM, 2003.

[33] "Intel oneAPI Math Kernel Library." https://software.intel.com/en-us/intel-mkl.

[34] T. Murayama, A. Muto, and A. Takei, "Convergence properties of iterative full-wave electromagnetic FEM analyses with node block preconditioners," IEICE Transactions on Electronics, vol.E101.C, pp.612–619, August 2018.

Toshio Murayama received the M.E. degree from the University of Tokyo in 1987, the M.S. degree from the University of California at Santa Barbara in 1991 and the Ph. D. degree in engineering from the University of Tokyo in 2012. He joined Sony Corporation in 1987. He has been researching numerical analysis of electromagnetics. His research interest convers also multi-domain circuit electromagnetic co-simulation.

Amane Takei received the B. E. and the M. E. degree from Hosei University in 1997 and 1999, respectively, and the Ph.D. of environmental study degree from The University of Tokyo in 2006. He has worked as Postdoctoral Fellow for The University of Tokyo from 2006 to 2010, and Associate professor for Tomakomai National Collage of Technology from 2010 to 2014. He is working as Associate Professor for Department of Electrical and systems Engineering, University of Miyazaki from 2014.